

# The extended use of actinometry in the interpretation of photochemical reaction engineering data

Cristina S. Zalazar, Marisol D. Labas, Carlos A. Martín, Rodolfo J. Brandi, Orlando M. Alfano, Alberto E. Cassano\*

INTEC, Universidad Nacional del Litoral and CONICET, Güemes 3450, (3000) Santa Fe., Argentina

Received 27 December 2004; received in revised form 14 March 2005; accepted 15 March 2005

## Abstract

Actinometry is an old and useful method developed in the chemistry field to estimate the amount of photons entering and being absorbed in a reaction cell filled with a well-known reacting system. As it is usually used it is of reduced suitability for intrinsic kinetic studies aimed at scaling-up purposes. However, in photochemical reaction engineering analysis it can be of invaluable help if it is properly applied to accurately calculate the boundary condition that is needed to solve the radiative transfer equation in laboratory photochemical reactors dedicated to obtain intrinsic kinetic parameters.

This contribution shows the way that actinometric measurements can be used as one of the most precise and simple methods to estimate the above mentioned boundary condition for both homogeneous and heterogeneous systems, an indispensable parameter to calculate with precise models based in the general radiation transport equation, the light distribution inside the reaction space. This local property is needed to formulate the initiation step of any photochemical reaction scheme when operation is made in the kinetic control regime. Consequently it will be always included in any properly developed complete reaction kinetic model. The proposed extended application is illustrated with one example employing a reactor used in photocatalytic reactions.

© 2005 Elsevier B.V. All rights reserved.

**Keywords:** Actinometry; Potassium ferrioxalate; Photochemical reaction; Photoreactor modelling

## 1. Introduction

More than 70 year ago research in photochemistry has introduced a very powerful tool with the name of actinometry. It consists in the use a well-known and simple chemical reaction – an actinometric reaction – with the ability to virtually “titrate” the number of photons that can be potentially absorbed in a given experimental apparatus. The idea behind the method is that knowing the change in concentration of the employed reactant or the developed product after a known time of irradiation, one can work backwards to calculate how many photons had entered the reactor to produce such result. In kinetics terms, under restricted concentrations and operating conditions, the rate of the employed reaction is exclusively a direct function of the rate of photon absorption

and almost independent of any other physico-chemical variable, including, to some extent, temperature. Thus, in general one can write to describe the rate of an actinometric reaction the following general equation:

$$R_{\lambda, \text{Act}}(x, t) = \nu_{\text{Act}} \Phi_{\lambda, \text{Act}} e_{\lambda, \text{Act}}^a(x, t) \quad \left\{ \begin{array}{l} C_1 \leq C \leq C_2 \\ \Delta C < \Delta C_{\text{fixed}} \\ T_1 \leq T \leq T_2 \\ \lambda_1 \leq \lambda \leq \lambda_2 \end{array} \right.$$

$\Phi_{\lambda, \text{Act}}$  known  
 $\rightarrow$  for each  
 given  $\lambda$ 
(1)

The stoichiometric coefficient,  $\nu_{\text{Act}}$ , in the most typical cases takes on the value of  $\pm 1$  depending upon the species (product or reactant) that is been considered. The

\* Corresponding author. Tel.: +54 342 4559176; fax: +54 342 4559185.  
E-mail address: acassano@ceride.gov.ar (A.E. Cassano).

**Nomenclature**

|                 |  |
|-----------------|--|
| $A$             | area [ $\text{cm}^2$ ]   |
| $C$             | concentration [ $\text{mole cm}^{-3}$ ]  |
| $e^a$           | local volumetric rate of photon absorption [einstein $\text{cm}^{-3} \text{s}^{-1}$ ]                                    |
| $E$             | radiant power [einstein $\text{s}^{-1}$ ]  |
| $F$             | spectral distribution of the output power from the lamp  |
| $G$             | incident radiation [einstein $\text{s}^{-1} \text{cm}^{-2}$ ]  |
| $h$             | Planck's constant [erg s]  |
| $\hat{i}$       | unit vector in the direction of the $x$ coordinate   |
| $I$             | specific intensity [einstein $\text{cm}^{-2} \text{s}^{-1} \text{sr}^{-1}$ ]   |
| $\bar{I}$       | especial specific intensity for single directional irradiation [einstein $\text{cm}^{-2} \text{s}^{-1} \text{sr}^{-1}$ ] |
| $L$             | length [cm]  |
| $N$             | total number of photons  |
| $n_i$           | number of moles of actinometer reactant or product   |
| $R$             | reaction rate [ $\text{mole s}^{-1} \text{cm}^{-3}$ ]  |
| $s$             | linear coordinate [cm]   |
| $T$             | temperature [K]  |
| $t$             | time [s]   |
| $V$             | volume [ $\text{cm}^3$ ]   |
| $x$             | rectangular Cartesian coordinate [cm]  |
| $\underline{x}$ | position vector [cm]   |

*Greek letters*

|                |  |
|----------------|--|
| $\alpha$       | molar Napierian absorptivity [ $\text{cm}^2 \text{mole}^{-1}$ ]            |
| $\delta$       | Dirac function   |
| $\phi$         | spherical coordinate [rad]   |
| $\Phi$         | overall quantum yield for the actinometer [mole einstein $^{-1}$ ]         |
| $\kappa$       | volumetric absorption coefficient [ $\text{cm}^{-1}$ ]                     |
| $\lambda$      | wavelength [nm]  |
| $\mu$          | $\cos \theta$ , dimensionless  |
| $\nu$          | frequency [ $\text{s}^{-1}$ ] or stoichiometric coefficient, dimensionless |
| $\theta$       | spherical coordinate [rad]   |
| $\sigma$       | volumetric scattering coefficient [ $\text{cm}^{-1}$ ]                     |
| $\Omega$       | solid angle [sr]   |
| $\hat{\Omega}$ | unit vector in the direction of propagation of radiation                   |

*Subscripts*

|     |  |
|-----|--|
| Abs | relative to absorbed                       |
| Act | relative to the actinometer                |
| Ox  | relative to the uranyl oxalate actinometer |
| $k$ | relative to species $k$                    |
| $R$ | relative to the reactor                    |
| $T$ | denotes total                              |
| Tot | denotes total in optical properties        |
| Tk  | relative to the tank                       |

|                |  |
|----------------|--|
| W              | relative to the wall of the reactor      |
| $\lambda$      | dependence on wavelength                 |
| $\hat{\Omega}$ | relative to the direction of propagation |
| 0              | initial condition                        |

*Superscripts*

|   |  |
|---|--|
| 0 | relative to the surface of radiation entrance or initial condition |
|---|--|

*Special symbol*

|     |                                |
|-----|--------------------------------|
| [=] | indicates “has unit of”        |
| —   | means average over wavelengths |

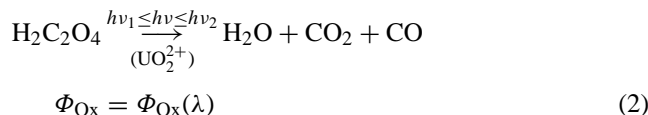
proportionality constant known as “overall quantum yield”,  $\Phi_{\lambda, \text{Act}}$ , is a function of wavelength but fairly constant within the prescribed ranges of concentrations, concentration changes and temperatures. Moreover, in some cases, the quantum yield is a weak function of wavelength and, in a first approximation, it could be possible (but not necessary) to work with an average value of  $\Phi$  for the whole range of  $\Delta\lambda$  where the actinometer absorbs radiation.  $e_{\lambda}^a(x, t)$  is the local volumetric rate of photon absorption (LVRPA), a function of wavelength and the concentration of all the radiation absorbing species present in the reaction space. In summary, under some unambiguously restricted experimental conditions, the reaction rate is a function of wavelength and the photon absorption rate as well as the typical spatial and temporal variables. There is no direct dependence on concentrations if, preserving the limits set for the operating conditions, those affecting the value of  $e_{\lambda}^a$  are not considered.

It is clear that, in principle, if we can calculate  $R_{\lambda, \text{Act}}(\underline{x}, t)$  from experimentally measured concentrations as a function of time, we should be able to calculate  $e_{\lambda}^a(\underline{x}, t)$  and with some additional work calculate the number of photons absorbed by the actinometer.

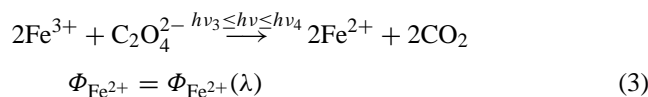
Many actinometric reactions have been proposed on account that there have been several objectives to accomplish, namely: (i) to use a simple and very reproducible reaction, (ii) to have a reaction with a well known quantum yield fairly constant in a defined range (sometimes narrow) of concentrations and temperatures (iii) to search for a tool covering different ranges of wavelengths, (iv) to carry out an intensive exploration for experimental conditions where a simple method to interpret the experimental data can be used and (v) to seek for reactions that can be used for liquid and gaseous systems.

Research in the chemistry field as reported for example by Noyes and Leighton [1], Calvert and Pitts [2], Rabek [3], Braun et al. [4] and Murov et al. [5], has solved most of these questions with very clever experimental proposals. Tribute should be paid to the original contributions to the two most commonly employed systems with this purpose in the work precisely described by Leighton and Forbes [6], Parkhurst

Brackett Jr. and Forbes [7], Forbes and Heidt [8], Volman and Seed [9] and Heidt et al. [10] for the uranyl oxalate decomposition and Parker [11], Hatchard and Parker [12] and Lee and Seliger [13] for the potassium ferrioxalate reaction. Up to 1992, according to the Handbook published by Murov et al. [5], 24 different reactions had been proposed with actinometric purposes. In spite of it, the uranyl oxalate and the potassium ferrioxalate, particularly the last, remain the most widely used. Essentially, under restricted concentrations and temperatures, the overall result of these two reactions is described as follows:



In this reaction the uranyl ion acts as a photosensitizer (it is the main radiation absorbing species but is not consumed) and the decomposition of the oxalic acid is usually followed by measuring its concentration before and after reaction with potassium permanganate titrations. The second and by far the most frequently employed actinometer is:



The amount of ferrous ion produced is measured via spectrophotometric measurement of the concentration of a complex formed with 1,10 phenanthroline at 510 nm.

Most of the literature in the chemistry field concentrates in the description of the experimental conditions under which, using polychromatic radiation, the rate of the number of photons entering the reaction vessel (and under those conditions, effectively absorbed by the actinometer) is:

$$N_{\sum \lambda} = \frac{[n_i(t=t) - n_i(t=0)]}{\bar{\Phi}_{\lambda, \text{Act}} t} [=] \text{einstein s}^{-1} \quad (4)$$

Strictly speaking, an equation such as Eq. (4) should be applied only for monochromatic radiation because absorption by the reactant (the reaction activation) and the quantum yield are not independent of wavelength. Consequently, its use may be restricted to a small wavelength interval or considered an approximation when used for wider polychromatic radiation fields (Note that in Eq. (4)  $\bar{\Phi}_{\lambda, \text{Act}}$  is an average value over wavelengths if polychromatic radiation is used). In spite of it, the value obtained from Eq. (4) is sometimes used to directly calculate the available photons for the reaction under study (different from the actinometric one), particularly when using an actinometer that absorbs in a range of wavelengths very similar to the one corresponding to the investigated reaction. A wide variety of experimental techniques and operating restrictions have been described to circumvent some of the difficulties associated with the quality of the results derived from the use of this very simple and practical expression [1–5]. The most important are:

1. To work under conditions of complete radiation absorption in all wavelengths. Then, all the arriving photons are counted.
2. To work with very small conversions. Then, from the radiation absorption point of view, the reactant concentration can be assumed constant and equal to the initial one and the possible effect on the radiation field resulting from absorption by the reaction products does not need to be taken into account.
3. For polychromatic radiation, to use an average overall quantum yield. Additionally, implicitly, the changes in the value of the reactant absorption coefficient with wavelength are ignored and overcome with the requirement of complete absorption at all wavelengths.

Sometimes, searching for more accurate information, to calculate the radiation entering the reaction cell and accounting for an incomplete radiation absorption in the existing optical thickness, the following equation has been proposed [2,4]:

$$N_{0, \sum \lambda} = \frac{[n_i(t=t) - n_i(t=0)]}{\bar{\Phi}_{\lambda, \text{Act}} t \{1 - \exp[-(\bar{\alpha}_{\lambda, \text{Act}})C_{\text{Act}}L]\}} [=] \text{einstein s}^{-1} \quad (5)$$

In this equation  $(\bar{\alpha}_{\lambda, \text{Act}})C_{\text{Act}}L$  is the optical thickness of the cell. Once more, this equation is strictly valid for monochromatic radiation, particularly because the incompleteness of radiation absorption may be a strong function of wavelength and the use of an average value of the quantum yield is usually an approximation. There is a singular exception to these – in our opinion – very practical but oversimplified ways of interpreting actinometric data and can be found in the contribution by Braun et al. [4]. Notwithstanding that finally, when the experimental techniques are discussed, after setting the required operating precautions and special warnings concerning polychromatic experiments, it is proposed the use of an equations very similar to Eqs. (4) or (5), the whole proposal of actinometer procedures is preceded by a more careful analysis of different possible alternatives under which the experiment can be performed. In this contribution, among the different discussed cases, a more detailed analysis is made, for example, of the particular condition when the concentration of the actinometer changes along the reaction evolution.

Equations such as (4) and (5) are mainly used in two different forms:

1. The absorbed photons resulting from Eq. (4) are transformed into an intensive property dividing the result by the reactor volume. The resulting value is directly used in the investigated system under the assumption that the same number of quanta per unit reactor volume will be absorbed in one (that is being studied) and the other (the actinometric) system.
2. Eq. (5) is used as a sort of boundary condition and the photons to be absorbed in the system under study are

calculated according to:

$$N_{\sum \lambda}^{\text{abs}} = N_{0, \sum \lambda} [1 - \exp(-\overline{\alpha_{\lambda}} C_i L)] \quad (6)$$

In Eq. (6)  $\overline{\alpha_{\lambda}}$  and  $C_i$  are the absorption coefficient and the concentration of the radiation absorbing species in the specific reaction under study for which the actinometric data ( $N_{0, \sum \lambda}$ ) were obtained. Once more the intensive character of the result is obtained dividing by the reactor volume. In other occasions equations such as (5) and (6) are written in terms of radiation fluxes (having units of einstein  $\text{cm}^{-2} \text{s}^{-1}$ ) dividing by the reactor window area. In these cases, after application of an equation analogous to Eq. (6), the volumetric rates are obtained dividing by the length of the reaction cell.

Using these equations, in all cases, more often than not, the data obtained from these global values of the photonic absorption rates are used in kinetic models, ignoring that these models always ask for point values of this function because the kinetic expression of any reaction should be written in local terms due to the intrinsic non uniformities of the existing radiation field.

## 2. A more rigorous and extensive approach

So far, one can see that several components of the reaction analysis have not been properly accounted for to obtain precise and meaningful values if the actinometric information is to be used with the objective of reaching an intrinsic quantitative kinetic result. Some of them have been treated with approximations and others with sometimes unnecessary restrictions in the experimental conditions. It is also important to realize that usually the used data correspond to global values for the whole reactor that are turned intensive in a very crude manner.

Perhaps, what is even more significant is the fact that actinometry is a much powerful tool if the experimental data are analyzed in a more precise way with some procedures derived from chemical reaction engineering analysis.

Conventional homogeneous actinometry without the help of photoreactor mathematical modeling does not account for the following points:

1. The ignored caution that, truly speaking, all these equations are valid for one-dimensional attenuation; i.e. they can be applied, for example, to a collimated, parallel beam of radiation or special reactor arrangements where one-dimensional models can be used (when the resulting radiation field is a function of a single coordinate along the penetration depth of the reactor). Sometimes, the radiation field may have significant gradients in more than one direction and consequently the radiative transfer equation is, at least in principle, three-dimensional.
2. The inappropriateness of the way used to derive intensive properties from global values and the direct use of these results in kinetic studies. This procedure does not take into account that the whole set of variables employed to build

kinetic models corresponds to local values; i.e., there are derived for a set of radiation absorption rates at each point inside the reactor, particularly because the radiation field is intrinsically non uniform; i.e., there is a whole field of reaction rates at each position inside the reaction space.

3. The need to use a proper averaging procedure of the kinetic model (the reaction rate) to analyze the experimental data that, by definition, in a well-mixed reactor, represent the result of the whole space having different local rates. Since it is almost impossible to have an isoactinic reactor (the analogous to an isothermal reactor in thermal kinetics) the non uniformities must be properly accounted for. Note that the differences in mixing and radiation transport characteristic times makes impossible to have a uniform radiation field when absorption and some times geometrical effects are present.
4. A precise consideration of polychromatic radiation that is the normal case in practical applications.
5. A precise account of reactant uneven radiation absorption at different wavelengths.
6. A precise use of the actinometer even if it does not completely absorbs all the arriving radiation in all the involved wavelengths of the experimental device.
7. A precise analysis of the results if the reaction is carried out beyond a very small initial conversion of the reactant; i.e., if the changes in concentration of reactant and product are not negligible.
8. The way that homogeneous actinometry can be very useful even in heterogeneous photoreactor kinetics studies. Conventional homogeneous actinometric methods cannot account for radiation scattering, but actinometry is still the best method to know the boundary condition of the Radiative Transfer Equation (RTE) for heterogeneous systems in laboratory reactors.
9. The way by which actinometric results obtained employing a lamp with a wide range of emission wavelengths (for example from 200 to 600 nm) can be used in a much restricted range of radiation absorption by the reactant (for example in photocatalysis with titanium dioxide, absorbing from 200 to 390 nm).

We think that actinometry is a very important tool in laboratory photochemical work but, at the same time that normally, its potentialities are not fully exploited to provide very useful and precise information. In our work we have been using actinometric measurements very often but with a single purpose: to know the absolute value and spectral distribution of the incident radiation arriving at the reactor window of radiation entrance (the boundary condition of RTE). With this information, then we solve the RTE inside the reaction space and we never need to make any sort of approximate extrapolation of the total radiation absorbed by the actinometer to a different reacting system (homogeneous or heterogeneous). Similarly, there is no need to obtain intensive properties of the photon absorption rate employing an approximation, before introducing the LVRPA into the kinetic model.

The actinometric result obtained with the appropriate experiments and a precise interpretation of the data usually provide an exact boundary condition for the solution of the RTE in the reaction cell and this is, in our opinion, the most important application of actinometry in reaction kinetics. We add to this analysis a method to account explicitly and more exactly for polychromatic irradiation. From this type of information we can provide an answer to all the above listed problems.

However, there are some questions that obviously actinometry cannot solve:

1. To provide information about the said boundary condition if the employed actinometer does not absorbs radiation in the complete wavelength range of interest.
2. To be used in models when it is necessary to consider the whole angular space of directions of radiation propagation because it does not provide information about the direction of the incoming rays. Directions of incidence can be obtained from radiation emission models [14]. In these cases, actinometer data can be used to verify the predicted, averaged value of the incident radiation (calculated over the total area of the windows of radiation entrance) and indirectly validate the results of the emission model. This procedure, with more or less difficulties, can be done regardless the geometry of the involved reactor.

It is important to note that for photoreactor design, in principle, we can never use actinometric measurements because the reactor has not been constructed yet and, consequently, measurements cannot be made. In this case, one must resort to emission models for the lamps and eventually reflectors [14] but unfortunately in this case one must rely on the information provided by the lamp's manufacturer concerning the total output power of the lamp and the spectral distribution of this output. When this information exists and the quality control of the lamp production is trustworthy, three-dimensional emission models are quite reliable. Matter-of-factly one can use especial actinometer devices to measure the lamp output if the manufacturer's information is not reliable, but carefully interpreted photometric measurements are simpler and faster. On the other hand, for laboratory experiments, we can use actinometers in a practical and accurate way and the only information that is needed is the quantitative spectral distribution (percentage or absolute) of the lamp output power (the emission curve or the emission lines). The method is facilitated even more if the total output power of the lamp is also accurately known.

Although we will show how actinometers can be used in heterogeneous systems, they are homogeneous reactions. Consequently we will make use of the RTE without scattering. We will also always consider that inside the reaction space there is no radiation emission.

The characteristics of radiation transport can be more easily seen from the definition of the fundamental quantity of the radiation field: the Spectral (monochromatic) Radiation

Intensity [15]:

$$I_{\Omega,\lambda}(\underline{x}, t) = \lim_{dA d\Omega dt d\lambda \rightarrow 0} \left( \frac{dE_{\lambda}}{dA \cos \theta d\Omega dt d\lambda} \right) \quad [ = ] \text{ einstein cm}^{-2} \text{ sr}^{-1} \text{ s}^{-1} \quad (7)$$

Hence, the Radiation Intensity depends not only on position and time, but also on the wavelength  $d\lambda$  about  $\lambda$  (that determine the energy of the transported photon) and direction characterized by the differential solid angle of directions  $d\Omega$  about the propagating direction  $\Omega$ . With this definition, the RTE in homogeneous and non emitting media is written as:

$$\frac{dI_{\lambda,\Omega}(\underline{x}, t)}{ds} = -\kappa_{\lambda}(\underline{x}, t) I_{\lambda,\Omega}(\underline{x}, t) \quad (8)$$

### 3. One dimensional, single direction radiation transport

Strictly speaking, only collimated (parallel) light beams can be safely modeled as one-dimensional and single directional systems. In this case, one needs a special definition of the light intensity to restrict the direction of propagation to a single direction ( $\Omega \rightarrow \underline{i}$ ) that coincides with one of the spatial coordinates. Here  $\underline{i}$  is the unit vector in the direction of the  $x$  coordinate. Then, for a one-dimensional and single directional model, the corresponding value of the intensity is obtained from:

$$I_{\lambda,\Omega}(x, t) = \bar{I}_{\lambda}(x, t) \delta(\Omega - \underline{i}) \quad (9)$$

Where  $\delta$ , the Dirac function is defined as:

$$\delta = \begin{cases} \int_{\Omega} \delta(\Omega - \underline{i}) d\Omega = 1 & \text{for } \Omega = \underline{i} \\ 0 & \text{for } \Omega \neq \underline{i} \end{cases} \quad (10)$$

In this case:

$$\bar{I}_{\lambda}(x, t) [ = ] \text{ einstein cm}^{-2} \text{ s}^{-1} \quad \text{with } \delta(\Omega - \underline{i}) [ = ] \text{ sr}^{-1}$$

The next important property in photochemistry is the incident radiation that is defined as:

$$G_{\lambda}(\underline{x}, t) = \int_{\Omega} I_{\lambda,\Omega}(\underline{x}, t) d\Omega [ = ] \text{ einstein cm}^{-2} \text{ s}^{-1} \quad (11)$$

$G_{\lambda}$  gives, at any point, all the radiation contributions from the whole space of directions. For one-dimensional and single directional irradiation, Eq. (11) results:

$$\begin{aligned} G_{\lambda}(x, t) &= \int_{\Omega} \bar{I}_{\lambda}(x, t) \delta(\Omega - \underline{i}) d\Omega = \bar{I}_{\lambda}(x, t) \int_{\Omega} \delta(\Omega - \underline{i}) d\Omega \\ &= \bar{I}_{\lambda}(x, t) \end{aligned} \quad (12)$$

The incident radiation is equal to the special (one-directional) specific intensity.



Up to now we have introduced one simplification: one-dimensional, single directional definitions and one deliberate restriction: monochromaticity. We will deal with polychromatic light further ahead. At present the question may be: Is the simplification an insurmountable difficulty that in practical terms can only be achieved with a complex train of optical devices to collimate the radiation beams? Alfano et al. [16–18] have shown that with the proper geometry and dimensions, a very good approximation to a one-dimensional radiation field can be achieved with a tubular lamp placed at the focal axis of a good quality parabolic reflector. When reflected radiation is significantly larger than direct radiation from the lamp, at a position separated a few centimeters from this device, the center part of the so generated radiation field is almost independent of the radial and angular coordinates. It will experience changes only along the distance traveled inside the reaction space when the reactor is placed perpendicular to the direction of the outgoing radiation beams (Fig. 1). This reactor may be considered a pseudo-one directional device. For laboratory reactors this is a very practical design for either homogeneous or heterogeneous systems even if for the second case some modifications may be advisable to simplify the solution of the required mathematical modeling. For both cases, the reactor, that could be a cylinder with two flat, parallel windows, is a one-dimensional flat plate that very closely behaves as having a single characteristic direction of radiation propagation. It is worthwhile to note that the very commonly used annular reactor may be treated with the one-dimensional approximation only in very special cases (when the reactor is very short, much shorter than the lamp length, the inner reactor wall is very close to the external wall of the lamp and the annular gap is small).

The absorbed radiation by component  $j$ , at every different point inside the reactor, in our notation, the local volumetric rate of photon absorption (LVRPA), is:

$$e_{\lambda,j}^a(x,t) = \kappa_{\lambda,j}(x,t) G_{\lambda}(x,t) \quad (13)$$

Note that this is a local value, the one that is required to incorporate the photonic absorption rate in any kinetic modeling.

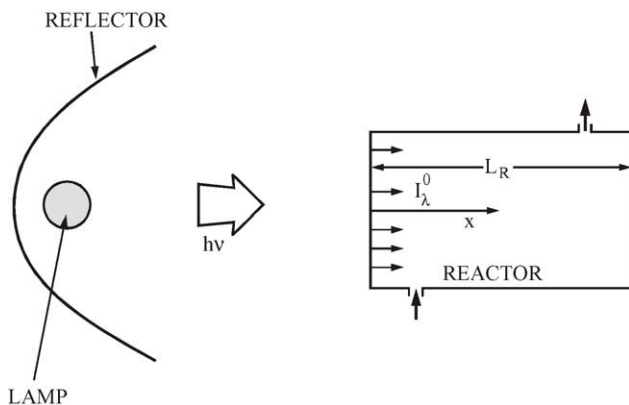


Fig. 1. One dimensional reactor with transparent window of radiation entrance.

It must be clearly remarked that in most of the reactor configurations (and almost always necessarily in heterogeneous systems where scattering is present) radiation transport is two-directional. In this particular contribution we are describing a very special type of reactor that is of general validity only for laboratory experiments and devices of the type described below.

#### 4. One-dimensional, single directional, monochromatic irradiation in homogeneous reactors

Actinometers are homogeneous reactions. Thus, unless a different situation is specified, we will be considering only absorption. For the one-dimensional, single directional case the RTE results:

$$\frac{dG_{\lambda}(x,t)}{dx} = -\kappa_{\lambda,\text{Tot}}(x,t)G_{\lambda}(x,t) \quad (14)$$

Let us now consider the case of one actinometer and make our exemplification with the potassium ferrioxalate reaction. Integrating Eq. (14) and combining with Eq. (13):

$$e_{\lambda}^a(x,t)|_{\text{Act}} = \kappa_{\lambda,j}(x,t)G_{\lambda,w} \exp \left[ - \int_0^x \kappa_{\lambda,\text{Tot}}(x,t) dx \right] \quad (15)$$

Here  $\kappa_{\lambda,j}$  is the absorption coefficient of the reactant (the potassium ferrioxalate) and  $\kappa_{\lambda,\text{Tot}}$  is the absorption coefficient of the complete reacting mixture (reactant and product).  $G_{\lambda,w}$  is the incident radiation impinging on the window of radiation entrance; i.e., the boundary condition. The reaction rate corresponding to the actinometer is:

$$R_{\lambda}(x,t)|_{\text{Fe}^{2+}} = \Phi_{\lambda,\text{Fe}^{2+}} e_{\lambda}^a(x,t)|_{\text{Act}} \quad (16)$$

$\Phi_{\lambda,\text{Fe}^{2+}}$  is the monochromatic overall quantum yield for the actinometer expressed in terms of the reaction product.

Combining Eq. (15) with Eq. (16) and writing the result in an explicit way for the potassium ferrioxalate reaction:

$$\begin{aligned} R_{\lambda}(x,t)|_{\text{Fe}^{2+}} &= \Phi_{\lambda,\text{Fe}^{2+}} \left[ \alpha_{\lambda}^{\text{Fe}^{3+}} C_{\text{Fe}^{3+}}(x,t) \right] G_{\lambda,w} \\ &\times \exp \left\{ - \int_0^x \left[ \alpha_{\lambda}^{\text{Fe}^{3+}} C_{\text{Fe}^{3+}}(x,t) + \alpha_{\lambda}^{\text{Fe}^{2+}} C_{\text{Fe}^{2+}}(x,t) \right] dx \right\} \quad (17) \end{aligned}$$

This is a local value of the reaction rate. If the reactor is well-mixed, concentrations are not a function of position but the distribution of radiation is. Thus, we need the average value of the reaction rate over the reactor volume to relate it with the change in concentration inside the reactor. For the one-dimensional, single directional reactor, in the homogeneous system, if the reactor is well mixed and the cross sectional area is constant, the average can be taken over the

reactor length:

$$\begin{aligned} & \langle R_\lambda(x, t) |_{\text{Fe}^{2+}} \rangle_{L_R} \\ &= \left\{ \Phi_{\lambda, \text{Fe}^{2+}} \left[ \underbrace{\alpha_\lambda^{\text{Fe}^{3+}} C_{\text{Fe}^{3+}}(t)}_{\kappa_{\lambda, \text{Fe}^{3+}}} \right] \underbrace{G_{\lambda, W}}_{\text{Boundary condition}} \right\} \frac{1}{L_R} \int_0^{L_R} \\ & \times \exp \left\{ - \left[ \underbrace{\alpha_\lambda^{\text{Fe}^{3+}} C_{\text{Fe}^{3+}}(t) + \alpha_\lambda^{\text{Fe}^{2+}} C_{\text{Fe}^{2+}}(t)}_{\kappa_{\lambda, \text{Tot}}} \right] x \right\} dx \end{aligned} \quad (18)$$

The result is:

$$\begin{aligned} & \langle R_\lambda(x, t) |_{\text{Fe}^{2+}} \rangle_{L_R} \\ &= \frac{\Phi_{\lambda, \text{Fe}^{2+}} G_{\lambda, W}}{L_R} \frac{\kappa_{\lambda, \text{Fe}^{3+}}(t)}{\underbrace{\kappa_{\lambda, \text{Fe}^{3+}}(t) + \kappa_{\lambda, \text{Fe}^{2+}}(t)}_{\kappa_{\lambda, \text{Tot}}(t)}} \\ & \times \{ 1 - \exp[-\kappa_{\lambda, \text{Tot}}(t)L_R] \} \end{aligned} \quad (19)$$

To complete the description of the reactor operation we need a mass balance. For kinetic studies searching for a better following-up of the reaction evolution, easiness of sampling and temperature control, we have found very convenient to use a recycling system made of the reactor, a pump, a heat exchanger and a rather large volume storage tank (Fig. 2). Under (i) isothermal conditions, (ii) large recirculating flowrate, (iii)  $V_R/V_T \ll 1$ , (iv) well mixing conditions and (v) small conversion per pass in the reactor, it can be shown that the following equation applies:

$$\langle R_\lambda(x, t) |_{\text{Fe}^{2+}} \rangle_{L_R} = \frac{V_R}{V_T} \frac{dC_{\text{Fe}^{2+}}}{dt} \Big|_{T_k} \quad (20)$$

A high recirculating flow rate is needed to ensure good mixing conditions and almost differential conversion per pass. Note that with the averaging procedure, the rate is an exclusive function of time; i.e.,  $R_\lambda(t) |_{\text{Fe}^{2+}}$  and that, according to the mass balance, changes in concentrations are measured in the tank. Inserting Eq. (19) into Eq. (20) the monochromatic boundary condition can be obtained after integration of:

$$\begin{aligned} \frac{dC_{\text{Fe}^{2+}}(t)}{dt} \Big|_{T_k} &= \frac{V_R}{V_T} \frac{G_{\lambda, W} \Phi_{\lambda, \text{Fe}^{2+}}}{L_R} \frac{\alpha_{\lambda, \text{Fe}^{3+}} [C_{\text{Fe}^{3+}}(t=0) - C_{\text{Fe}^{2+}}(t)]}{\alpha_{\lambda, \text{Fe}^{3+}} [C_{\text{Fe}^{3+}}(t=0) - C_{\text{Fe}^{2+}}(t)] + \alpha_{\lambda, \text{Fe}^{2+}} C_{\text{Fe}^{2+}}(t)} \\ & \times \underbrace{\{ 1 - \exp[-\alpha_{\lambda, \text{Fe}^{3+}} [C_{\text{Fe}^{3+}}(t=0) - C_{\text{Fe}^{2+}}(t)] - \alpha_{\lambda, \text{Fe}^{2+}} C_{\text{Fe}^{2+}}(t)] L_R \}}_A \end{aligned} \quad (21)$$

This equation cannot be solved analytically. However, experimentally we have values of  $C_{\text{Fe}^{2+}}$  versus time.  $C_{\text{Fe}^{3+}}^0$  and all absorptivities can be known as well as the quantum

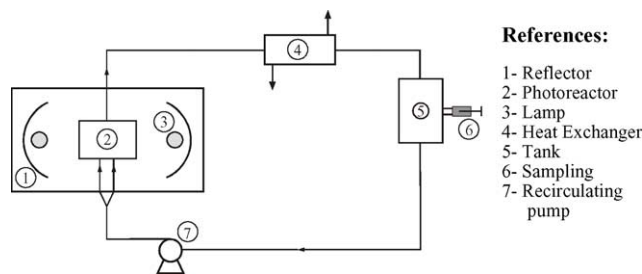


Fig. 2. The recycling system.

yield, and the reactor and total volumes together with the reactor length are also known values. The only unknown left is  $G_{\lambda, W}$ . With a non-linear single parameter estimation this value can be easily obtained because we must only compare experimental time rates of change of the  $C_{\text{Fe}^{2+}}$  values with predictions from the solution of Eq. (21). Needless is to say that the extent of the reaction cannot be carried out beyond the point for which the value of the overall quantum yield remains constant. However, this is not a serious limitation because the constancy of the quantum yield is known to persist in a rather wide range of ferric salts concentrations [5]. Summarizing, Eq. (21) is an exact expression if: (i) propagation of radiation can be assumed one-dimensional and single directional, (ii) the reactor is well mixed, (iii) the wavelength of the energy emitted by the lamp for which calculation is made falls within the wavelength range of absorption by the actinometric solution and (iv) the extent of the reaction is carried out till the limit in which the monochromatic overall quantum yield of the actinometer solution is known to remain constant for the involved wavelength.

Using potassium ferrioxalate, the problem is even simpler because when working with a wavelength not larger than 430 nm, not too low actinometer concentrations and an optical path not shorter than 5 cm, during the first part of the reaction performed under these circumstances, the time derivative is a straight line. This can be easily shown because according to Hatchard and Parker [12] under these conditions the term labeled with A is close to 1 due to the very high absorption produced by the potassium ferrioxalate. Moreover, at the initial stages of the reaction the term  $\alpha_{\text{Fe}^{2+}} [C_{\text{Fe}^{2+}}(t)]$  can be neglected compared with  $\alpha_{\text{Fe}^{3+}} [C_{\text{Fe}^{3+}}(t=0)] - \alpha_{\text{Fe}^{3+}} [C_{\text{Fe}^{2+}}(t)]$ . Hence:

$$\lim_{t \rightarrow 0} \underbrace{\left( \frac{dC_{\text{Fe}^{2+}}(t)}{dt} \Big|_{T_k} \right)}_{\text{EXPERIMENTS}} = \frac{V_R}{V_T} \frac{G_{\lambda, W} \Phi_{\lambda, \text{Fe}^{2+}}}{L_R} \quad (22)$$

When the above conditions are fulfilled, Eq. (22) is a valid simplification and  $G_{\lambda,W}$  can be easily obtained from it because the plot of  $C_{\text{Fe}^{2+}}$  versus  $t$  is always a straight line. When this linearity is not observed the complete Eq. (21) must be used.

An important consideration has been stated: the well stirred reactor operation. The hydrodynamic mixing “characteristic time” and the photon transport “characteristic time” are so much different that the hydrodynamics of the flow field does not affect per se the light distribution inside the reactor. However, if the distribution of the concentration of the radiation absorbing species is affected by the flow field, it must be taken into account resorting to a precise modeling of the mass balance and its coupling with the radiation balance. It is clear that, in this case, the mass balance will ask for information concerning the spatial distribution of the field of velocities. In the proposed methods for laboratory reaction kinetics studies, this problem does not exist because we impose on the experimental procedure the perfect mixing operating condition.

It is clear that from Eq. (22) one can obtain immediately the incident radiation at the entrance of the reactor window. Knowing  $G_{\lambda,W}$ , there is no need to assume that the same amount of photons absorbed by the actinometer will be absorbed by the chemical system under study. Thus, using the same reactor, for any other homogeneous reaction employing reactant  $k$  for example, we can know the spatial distribution of photon absorption rates, according to:

$$e_{\lambda}^a(x, t)|_k = \kappa_{\lambda,k}(x, t) G_{\lambda,W} \exp[-\kappa_{\lambda,\text{Tot}}(t)x] \quad (23)$$

$$G_{\lambda,W} = \frac{V_T}{V_R} \frac{L_R}{\Phi_{\lambda,\text{Fe}^{2+}} t} \left\{ C_{\text{Fe}^{2+}} + \frac{1}{\alpha_{\text{Fe}^{3+}} L_R} \left[ \frac{1 - \exp[-\alpha_{\text{Fe}^{3+}} C_{\text{Fe}^{3+}}(t=0) L_R]}{1 - \exp[-\alpha_{\text{Fe}^{3+}} (C_{\text{Fe}^{3+}}(t=0) - C_{\text{Fe}^{2+}}) L_R]} \right] \right\} \quad (26)$$

Eq. (23) includes the case of the existence of any form of inner filtering effect. It is taken into account when  $\kappa_{\lambda,\text{Tot}}$  is calculated; i.e., it comprises the absorption coefficient of the remaining reactant absorbing species plus any other species (a product, for example) that absorbs radiation in the wavelength under consideration. This procedure can be done when the measurement of the actinometer is made with the same wavelength that will be used by the reaction under study.

It is also important to recall that Eq. (23) produces a local value, i.e., a function of position. This local value is needed to calculate the initiation step of a photochemical reaction at every point inside the reactor space. Then, it will be included in any kinetic model derived from a reaction scheme or mechanism. For example, under isothermal and well mixing conditions:

$$R_{\lambda,k}(x, t) = F[C_1(t), C_2(t) \dots C_n(t), e_{\lambda}^a(x, t)] \quad (24)$$

The reaction rate of species  $k$  must be incorporated into the mass balance of the experimental reactor. However, even in well mixed reactors, before integrating the mass balance equation, we must always calculate the spatial average of the reaction rate [as indicated for example by Eq. (18)], because  $e_{\lambda}^a$  is an irreducible function of position. Calculating this average for the whole reactor volume may be more or less complicated according to the derived kinetic model and the type of reactor that is used. For flat reactors as the one adopted in this example, in the worst case, we will face a simple numerical integration that can be accomplished with standard commercial programs. The same commentary applies for the solution of the mass balance in the proposed operating system.

There is an important point to note. A similar (not equal) equation to Eq. (22) is used in the chemistry literature. It implies that at the employed wavelength radiation absorption is complete. On the contrary, Eq. (21) does not have this limitation. Moreover, working with low conversion, Eq. (21) can be simplified and used under conditions of incomplete absorption because absorption by ferrous salts can be neglected rendering:

$$\begin{aligned} & \left. \frac{dC_{\text{Fe}^{2+}}(t)}{dt} \right|_{T_k} \\ &= \frac{V_R}{V_T} \frac{L_R}{L_R} G_{\lambda,W} \Phi_{\lambda,\text{Fe}^{2+}} \\ & \times \{1 - \exp[-\alpha_{\text{Fe}^{3+}} [C_{\text{Fe}^{3+}}(t=0) - C_{\text{Fe}^{2+}}(t)]] L_R\} \end{aligned} \quad (25)$$

Integrating Eq. (25), we can extract directly the value of  $G_{\lambda,W}$ :

Note that for very high radiation absorption, Eq. (26) reduces to Eq. (22).

## 5. One-dimensional, single directional, polychromatic irradiation in homogeneous systems

Equations such as Eqs. (21), (22) and (26) can be used with polychromatic radiation. Eq. (21) or eventually Eq. (26) must be used when there is no complete absorption by the actinometer. We will illustrate the procedure with Eq. (22) because of its simplicity, thus facilitating the conceptual approach. Hence, for polychromatic light in the wavelength range from  $\lambda_1$  to  $\lambda_2$ , low conversions and complete absorption for all the wavelengths of emission by the lamp, we have:

$$\left( \frac{V_T}{V_R} \right) \lim_{t \rightarrow 0} \frac{\Delta C_{\text{Fe}^{2+}}}{\Delta t} \Big|_f d\lambda = \frac{1}{L_R} \int_{\lambda_1}^{\lambda_2} \Phi_{\lambda,\text{Fe}^{2+}} G_{\lambda,W} d\lambda \quad (27)$$



The integral of the right hand side of Eq. (27) will be performed numerically with some form of discretization of the wavelength interval [19]. When the lamp has emission lines, it can be supposed that there are as many monochromatic reactors as emission lines and add up the effects of each pseudo-monochromatic reactor. When the emission is continuous one can divide the whole wavelength interval into several discrete regions of emission and proceed with the same concept.

Eq. (27) can be rearranged to give:

$$\begin{aligned} \left(\frac{V_R}{V_T}\right) \lim_{t \rightarrow 0} \frac{\Delta C_{Fe^{2+}}}{\Delta t} \Big|_{f, d\lambda} &= \frac{G_{Tot,W}}{L_R} \int_{\lambda_1}^{\lambda_2} \Phi_{\lambda, Fe^{2+}} \frac{E_{\lambda}}{E_{Tot}} d\lambda \\ &= \frac{G_{Tot,W}}{L_R} \int_{\lambda_1}^{\lambda_2} F_{\lambda} \Phi_{\lambda, Fe^{2+}} d\lambda \end{aligned} \quad (28)$$

$F_{\lambda}$  is generally known from the lamp manufacturer; it gives the spectral distribution of the output power from the lamp. Then, it is possible to calculate from experiments the value of  $G_{Tot,W}$  and obtain afterwards, using again  $F_{\lambda}$ , the spectral distribution of the incident radiation at the reactor window.

$$G_{\lambda, W} = \frac{L_R F_{\lambda}}{\sum_{\lambda_1}^{\lambda_2} (\Phi_{\lambda, Fe^{2+}} + F_{\lambda})} \left(\frac{V_T}{V_R}\right) \left\{ \underbrace{\lim_{t \rightarrow 0} \frac{\Delta C_{Fe^{2+}}}{\Delta t} \Big|_{f, d\lambda}}_{\text{EXPERIMENTS}} \right\} \quad (29)$$

$G_{\lambda, W}$  is the spectral distribution of the incident radiation arriving at the reactor window. The same considerations made before concerning incomplete absorption or not too small conversions are valid for polychromatic radiation. In these cases, with more complex equations, we need the spectral distribution of the absorption coefficient of the ferric and ferrous salts ( $\alpha_{Fe^{3+}}$  and  $\alpha_{Fe^{2+}}$ ) that can be easily obtained with spectrophotometric measurements. The biggest problem that one will encounter is that a numerical integration will be needed. Cabrera et al. [20] and Martín et al. [21], have successfully used these approaches for polychromatic radiation.

## 6. One-dimensional, polychromatic reactors in heterogeneous systems

In heterogeneous systems the solution of the radiative transfer equation is more complex because we must include

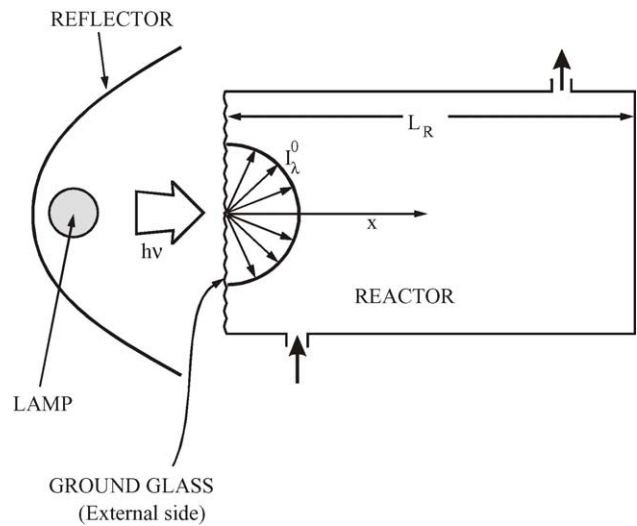


Fig. 3. Reactor with a window producing diffuse radiation entrance inside the reactor.

scattering. However, the same reactor described before, with a slight modification can be used, furnishing for laboratory reactors the simplest solution for a rigorous treatment of the RTE. To simplify the interpretation of the experimental data Cabrera et al. [20] have proposed to use a diffuse boundary condition at the windows of radiation entrance. It is simple to see the advantage of this experimental modification if one compares the general RTE:

$$\begin{aligned} \frac{dI_{\lambda, \underline{\Omega}(\theta, \phi)}(x, t)}{ds} &= - \underbrace{[\kappa_{\lambda}(x, t) + \sigma_{\lambda}(x, t)] I_{\lambda, \underline{\Omega}(\theta, \phi)}(x, t)}_{\text{ABSORPTION AND OUT SCATTERING}} \\ &+ \underbrace{\frac{\sigma}{4\pi} \int_0^{4\pi} I_{\lambda, \underline{\Omega}'(\theta, \phi)}(x, t) p[\underline{\Omega}'(\theta, \phi) \rightarrow \underline{\Omega}(\theta, \phi)] d\Omega'}_{\text{IN SCATTERING}} \end{aligned} \quad (30)$$

with the RTE of one-dimensional model:

$$\begin{aligned} \mu \frac{\partial I_{\lambda, \mu}(x, t)}{\partial x} + [\kappa_{\lambda}(x, t) + \sigma_{\lambda}(x, t)] I_{\lambda, \mu}(x, t) \\ = \frac{\sigma_{\lambda}}{2} \int_{\mu=-1}^{\mu=1} I_{\lambda, \mu'}(x, t) p(\mu' \rightarrow \mu) d\mu' \end{aligned} \quad (31)$$

In Eq. (30)  $\theta$  and  $\phi$  are the angles that define the solid angle of radiation propagation in a spherical coordinate system. In Eq. (31)  $\mu = \cos \theta$  and we need a single directional variable to characterize the propagation of radiation. In addition, a diffuse boundary condition produces azimuthal symmetry; i.e., diffuse radiation entrance produced by this special reactor window allows us to assume that radiation intensities going inside the reactor are equal for all directions (Fig. 3). In other words, as usual, in these equations we need the incoming radiation (the boundary condition). In Eq. (30), the incoming

radiation will be of the type  $I_{\lambda}^0(\theta, \phi)$ , whereas in the second case we just need  $I_{\lambda}^0 \neq I_{\lambda}^0(\theta, \phi)$ .

The experimental simplification rendering azimuthal symmetry facilitates in great manner the solution of the RTE when scattering is present [20–22]. How difficult is to obtain this special boundary condition in a laboratory reactor? The solution is very simple: the external side of the reactor windows must be made of ground glass or quartz. Note very clearly that without this modification in the radiation entrance boundary condition, photoreactors with radiation scattering, must always be modeled as two-directional.

The boundary condition, in laboratory reactors having this modification, can also be obtained with actinometric methods. In this particular case, even for homogeneous actinometry in one-dimensional reactors, the Lambert-Beer equation has some changes [15]. According to Brandi et al. [23] it is possible to work as follows:

$$\mu \frac{dI_{\lambda, \mu}(x, t)}{dx} + \kappa_{\lambda, \text{Tot}}(x, t) I_{\lambda, \mu}(x, t) = 0 \quad (32)$$

with  $I_{\lambda, \mu}(0, t) = I_{\lambda}^0 \neq f(\mu)$

Integrating Eq. (32) for a well-mixed reactor:

$$I_{\lambda, \mu}(x, t) = I_{\lambda}^0 \exp \left[ -\frac{\kappa_{\lambda, \text{Tot}}(t)}{\mu} x \right] \quad (33)$$

Using the potassium ferrioxalate actinometer, the LVRPA becomes:

$$\begin{aligned} e_{\lambda}^a(x, t)|_{\text{Act}} &= 2\pi \kappa_{\lambda, \text{Fe}^{3+}}(t) \int_0^1 I_{\lambda, \mu'}(x, t) d\mu' \\ &= 2\pi \kappa_{\lambda, \text{Fe}^{3+}}(t) I_{\lambda}^0 E_2[\kappa_{\lambda, \text{Tot}}(t)x] \end{aligned} \quad (34)$$

In Eq. (34),  $E_2$  is the second order exponential integral function [24]. The exponential integral function of  $n$ th order is defined as:

$$E_n(z) = \int_0^1 \mu^{n-2} \exp \left[ -\frac{z}{\mu} \right] d\mu \quad (35)$$

Considering again a recirculating batch reactor, the reaction indicated by Eq. (16) and the mass balance of Eq. (20), the reaction rate gives:

$$\langle R_{\lambda}(x, t) \rangle_{L_R} = \frac{dC_{\text{Fe}^{2+}}(t)}{dt} \Big|_{\text{Act}} \left( \frac{V_T}{V_R} \right) = \Phi_{\lambda, \text{Fe}^{2+}} \langle e_{\lambda}^a \rangle_{\text{Act}/L_R} \quad (36)$$

### 6.1. Case a: complete absorption at the wavelength under consideration

For simplicity, we will analyze this case for monochromatic radiation. Considering low conversions, it may be assumed that  $\kappa_{\lambda, \text{Tot}} = \kappa_{\lambda, \text{Fe}^{3+}}$ . With this standard restriction, after substitution of Eq. (34) let us integrate Eq. (36) to

calculate the reactor length averaged LVRPA.

$$\begin{aligned} \langle e_{\lambda}^a \rangle_{\text{Act}/L_R} &= \frac{1}{L_R} \int_0^{L_R} e_{\lambda}^a|_{\text{Act}} dx \\ &= \frac{1}{L_R} 2\pi \kappa_{\lambda, \text{Fe}^{3+}}(t) I_{\lambda}^0 \int_0^{L_R} E_2[\kappa_{\lambda, \text{Tot}}(t)x] dx \\ &= \frac{\pi I_{\lambda}^0 \kappa_{\lambda, \text{Fe}^{3+}}(t)}{L_R \kappa_{\lambda, \text{Tot}}(t)} \end{aligned} \quad (37)$$

The last result follows because:

$$\int E_n(z) dz = -E_{n+1}, \quad E_3(0) = 1/2 \quad \text{and} \quad \lim_{z \rightarrow \infty} E_3(z) \rightarrow 0$$

The last approximation can be applied because the product  $\kappa_{\lambda, \text{Tot}} \times L_R$  is large enough to ensure complete absorption. Working with low conversion, makes sure that absorption by the ferrous ion is negligible and absorption by the ferric salt is well defined. Once more, the plot of  $\text{Fe}^{+2}$  concentration versus time gives a straight line; then, the value of the light intensity that is needed for the solution of the RTE in the heterogeneous system, is obtained from:

$$I_{\lambda}^0 = \frac{L_R}{\pi \Phi_{\lambda, \text{Fe}^{2+}}} \left( \frac{V_T}{V_R} \right) \underbrace{\left\{ \lim_{t \rightarrow t_0} \left( \frac{\Delta C_{\text{Fe}^{2+}}}{\Delta t} \right) \right\}}_{\text{Experiments}} \quad (38)$$

It may be convenient to point out that the solution of the RTE in slurry photocatalytic reactors, even in one-dimensional diffuse boundary condition models, is always obtained integrating intensities. That is why we have not used here equations in terms of the Incident Radiation.

### 6.2. Case b: incomplete absorption in some wavelengths

Consider the case of the same reactor as before (one dimensional, diffuse radiation entrance, isothermal, batch in the recirculation mode and well-mixed). To get some improvement in the uniformity of the radiation field in the reaction space, we will irradiate the cylinder from both flat windows as indicated in Fig. 4 [25]. In this case, we face the following problem: the employed lamp is polychromatic and emits significant radiation between 275 and 580 nm, a wavelength range for which the actinometer do not have complete absorption in all the significant wavelengths. However, the overall quantum yield as a function of wavelength is known in the above mentioned spectral interval. Moreover, in this case, the research project was interested in knowing the entering energy to the reactor as a function of wavelength (and not only the total entering energy). This information was required to use the correct boundary condition for a photocatalytic system. In this case it was needed to select from all the wavelengths of emission by the lamp, only those energies corresponding to the wavelength interval of absorption by titanium dioxide in the used reactor (between 275 and 385 nm). This permits to use the energy

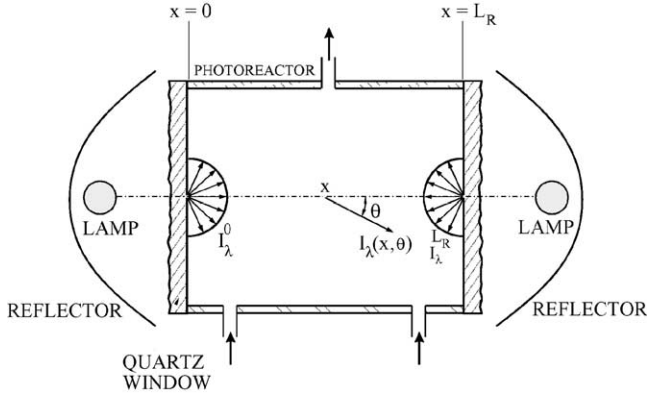


Fig. 4. One dimensional-one directional reactor irradiated from both sides.

corresponding to the restricted range of absorption by the catalyst in the boundary condition required in the solution of the RTE for the heterogeneous system.

Integrating Eq. (32) for the case in which both windows are irradiated:

$$I_{\lambda,\mu}(x,t) = I_{\lambda}^0 \left[ \exp\left(-\frac{\kappa_{\lambda,\text{Tot}}(t)x}{\mu}\right) + \exp\left(-\frac{\kappa_{\lambda,\text{Tot}}(t)(L_R-x)}{\mu}\right) \right] \quad (39)$$

The LVRPA becomes:

$$e_{\lambda}^a(x,t)|_{\text{Act}} = 2\pi \kappa_{\lambda,\text{Fe}^{3+}}(t) \int_{\mu=-1}^{\mu=1} I_{\lambda,\mu'}(x,t) d\mu' \quad (40)$$

Then:

$$\begin{aligned} e_{\lambda}^a(x,t)|_{\text{Act}} &= 2\pi \kappa_{\lambda,\text{Fe}^{3+}}(t) \int_{-1}^1 I_{\lambda,\mu'}(x,t) d\mu' \\ &= 2\pi \kappa_{\lambda,\text{Fe}^{3+}}(t) I_{\lambda}^0 \\ &\quad \times [E_2(\kappa_{\lambda,\text{Tot}}(t)x) + E_2(\kappa_{\lambda,\text{Tot}}(t)(L_R-x))] \end{aligned} \quad (41)$$

Again, the average value of the LVRPA is needed:

$$\begin{aligned} \langle e_{\lambda}^a|_{\text{Act}} \rangle_{L_R} &= \frac{1}{L_R} \int_0^{L_R} e_{\lambda}^a(x,t)|_{\text{Act}} dx \\ &= \frac{1}{L_R} 2\pi \kappa_{\lambda,\text{Fe}^{3+}}(t) I_{\lambda}^0 \int_0^{L_R} \\ &\quad \times [E_2(\kappa_{\lambda,\text{Tot}}(t)x) + E_2(\kappa_{\lambda,\text{Tot}}(t)(L_R-x))] dx \end{aligned} \quad (42)$$

Integrating:

$$\begin{aligned} \langle e_{\lambda}^a|_{\text{Act}} \rangle_{L_R} &= \frac{1}{L_R \kappa_{\text{Tot}}} 2\pi \kappa_{\lambda,\text{Fe}^{3+}}(t) I_{\lambda}^0 \\ &\quad \times 2 [E_3(0) - E_3(\kappa_{\lambda,\text{Tot}} L_R)] \end{aligned} \quad (43)$$

To compute the incident radiation, we recall that the entering radiation is diffuse:

$$\begin{aligned} G_{\lambda,W} &= \int_{\Omega} I_{\lambda,\Omega(\theta,\phi)}(x,t) d\Omega \\ &= \underbrace{2\pi}_{\text{Due to azimuthal symmetry}} \int_{\theta=0}^{\theta=\pi/2} I_{\lambda,\theta}(x,t) \sin\theta d\theta = 2\pi \int_0^1 I_{\lambda}^0 d\mu \\ &= 2\pi I_{\lambda}^0 \end{aligned} \quad (44)$$

Combining Eqs. (43) and (44):

$$\langle e_{\lambda}^a|_{\text{Act}} \rangle_{L_R} = \frac{2G_{\lambda,W} \kappa_{\lambda,\text{Fe}^{3+}}(t)}{L_R \kappa_{\lambda,\text{Tot}}} [E_3(0) - E_3(\kappa_{\lambda,\text{Tot}} L_R)] \quad (45)$$

Eq. (45) must be inserted into the mass balance. Recalling the value of  $E_3(0)$ :

$$\begin{aligned} \left( \frac{V_T}{V_R} \right) \left[ \frac{dC_{\text{Fe}^{2+}}(t)}{dt} \right]_{\lambda} \\ = \Phi_{\lambda,\text{Fe}^{2+}} \frac{\kappa_{\lambda,\text{Fe}^{3+}}}{\kappa_{\lambda,\text{Tot}}} \frac{G_{\lambda,W}}{L_R} \left[ \frac{1}{2} - E_3(\kappa_{\lambda,\text{Tot}} L_R) \right] \end{aligned} \quad (46)$$

Eq. (46) is valid for monochromatic radiation. However the experimental measurement of the change in the ferrous salt concentration is the result of polychromatic radiation. It can be accepted that the wavelength distribution arriving at the reactor windows is the same than that corresponding to the lamp emission (furnished by the lamp manufacturer) with all quantities expressed in photochemical units for energies [recall the spectral distribution of the lamp output used in Eq. (28)]:

$$G_{\lambda,W} = \frac{E_{\lambda}}{E_{\text{Tot}}} G_{\text{Tot},W} = F_{\lambda} G_{\text{Tot},W} \quad (47)$$

Substituting into Eq. (46):

$$\begin{aligned} G_{\text{Tot},W} &= \left( \frac{V_T}{V_R} \right) \underbrace{\left[ \frac{dC_{\text{Fe}^{2+}}(t)}{dt} \right]_{\int \lambda d\lambda}}_{\text{Experiments}} \\ &\quad \times \frac{1}{\frac{2}{L_R} \sum_{\lambda} \Phi_{\lambda,\text{Fe}^{2+}} \frac{\kappa_{\lambda,\text{Fe}^{3+}}}{\kappa_{\lambda,\text{Tot}}} \frac{E_{\lambda}}{E_{\text{Tot}}} \left[ \frac{1}{2} - E_3(\kappa_{\lambda,\text{Tot}} L_R) \right]} \end{aligned} \quad (48)$$

With low conversion and using the previously mentioned straight line plot:

$$G_{\text{Tot,W}} = \left( \frac{V_T}{V_R} \right) \frac{1}{\frac{2}{L_R} \sum_{\lambda=275}^{\lambda=580} \Phi_{\lambda, \text{Fe}^{2+}} \frac{E_{\lambda}}{E_{\text{Tot}}} \left[ \frac{1}{2} - E_3(\kappa_{\text{Fe}^{3+}} L_R) \right]} \times \lim_{t \rightarrow t_0} \underbrace{\left[ \frac{C_{\text{Fe}^{2+}}}{t - t_0} \right]_{\sum \lambda}}_{\text{Experiments}} \quad (49)$$

And using again Eq. (47), the incident radiation, as a function of wavelength can be obtained. With Eq. (44), the incoming intensities ( $I_{\lambda}^0$ ) as a function of wavelength can be immediately calculated. With this boundary condition we can proceed to solve Eq. (31) for the heterogeneous system.

In these equations we have assumed that both lamps have exactly the same radiation output. When the difference between the boundary conditions on the right and the left side of the reactor is significant, it is always possible to use a very similar equation adding the two different contributions from both sides. The resulting expression does not add significant additional complexity, but two different actinometric measurements (one for each lamp, separately) will be necessary.

## 7. Application

As an illustrative example of these procedures, we will show the case of diffuse irradiation with a lamp with emission in a wavelength range where the actinometer does not have complete absorption and the values of  $I_{\lambda}^0$  are needed in a restricted wavelength interval.

Consider the case of a Philips HPA 1000 lamp with significant emission in the wavelength range between 275 and 580 nm (Fig. 5). No information is provided concerning the total output power, but the normalized percentage distribution of the output power as a function of wavelength is known

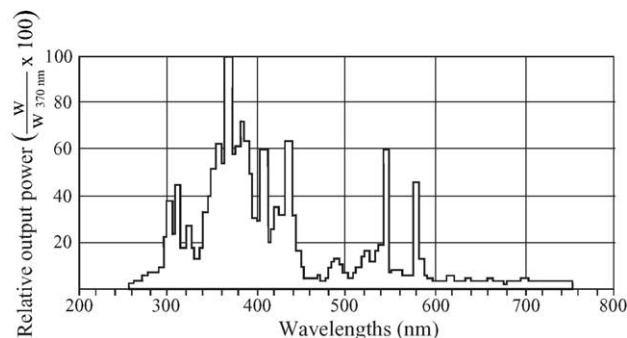


Fig. 5. Spectral distribution of the lamp output power (Philips HPA 1000).

(in terms of  $E/E_{\text{max}}$ , with  $E_{\text{max}}$  being the 100% output power at 370 nm). Note that the ratio of  $E/E_{\text{max}}$  in W is not equal to the ratio of  $E/E_{\text{max}}$  in einstein because of the wavelength dependence involved in the transformation [4]. Table 1 indicates the calculations that must be done to report the relative output power in terms of the power in einstein  $\text{s}^{-1}$  at a given wavelength with respect to the total power in the same units. Table 2, gives the values that must be used to apply Eq. (49). In this case the actinometer (potassium ferrioxalate) concentration was 0.021 M. The values of quantum yields were taken from Calvert and Pitts [2], Braun et al. [4] and Murov et al. [5] and the molar absorptivities were taken from the last two. The reactor length  $L_R$  was equal to 5.2 cm and the ratio of  $V_T/V_R$  was equal to 45.29 (a storage tank was included in the recirculating system).

Fig. 6, shows the experimental results from which the limit required by Eq. (49) can be calculated. Table 3 shows the numerical values. There are values for each one of the lamps (both lamps are not identical) and also the results obtained interposing neutral density filters between the lamps and the reactor. Table 4 shows the values obtained calculating the incident radiation in each condition. Finally from this results and the distribution of the output power given in Table 1, the desired values of the incoming intensities in the wavelength

Table 1  
Relative output power in terms of the energy in einstein  $\text{s}^{-1}$  as a function of wavelength

| $\lambda_i$ (nm) | $E_{\lambda}^*/E_{\text{max}}^*$ (W/W $\times 10^2$ ) | $\lambda_i/\lambda_{\text{max}}$ | $E_{\lambda}/E_{\text{max}}$ (einstein/einstein $\times 10^2$ ) | $E_{\lambda}/E_{\text{total}}$ (einstein/einstein $\times 10^2$ ) |
|------------------|---|----------------------------------|---|---|
| 275              | 10.0  | 0.74                             | 7.43  | 1.04  |
| 305              | 37.5  | 0.82                             | 30.91   | 4.31  |
| 310              | 45.0  | 0.84                             | 37.70   | 5.26  |
| 324              | 27.0  | 0.88                             | 23.64   | 3.30  |
| 359              | 63.0  | 0.97                             | 61.13   | 8.52  |
| 370              | 100.0   | 1.00                             | 100.00  | 13.90   |
| 385              | 72.0  | 1.04                             | 74.92   | 10.40   |
| 410              | 60.0  | 1.11                             | 66.49   | 9.27  |
| 423              | 35.0  | 1.14                             | 40.01   | 5.58  |
| 436              | 64.0  | 1.18                             | 75.42   | 10.50   |
| 490              | 12.5  | 1.32                             | 16.55   | 2.31  |
| 523              | 17.0  | 1.41                             | 24.03   | 3.35  |
| 545              | 60.0  | 1.47                             | 88.38   | 12.30   |
| 580              | 45.0  | 1.57                             | 70.54   | 9.84  |

Where:  $\lambda_i$  is the wavelength of emission peak  $i$ ,  $E_{\lambda}^*/E_{\text{max}}^*$  is the relative output power in terms of W,  $\lambda_i/\lambda_{\text{max}}$ : wavelength relationship with respect to that of maximum emission,  $E_{\lambda}/E_{\text{max}}$ : is the relative output power in terms einstein obtained as  $(E_{\lambda}^*/E_{\text{max}}^*) \times (\lambda_i/\lambda_{\text{max}})$ ,  $\frac{E_{\lambda}}{E_{\text{Total}}} = (E_{\lambda}/E_{\text{max}}) / \left( \sum_{\lambda=275}^{\lambda=580} E_{\lambda}/E_{\text{max}} \right)$ .

Table 2  
Values used in Eq. (49)

| $\lambda$ (nm) | $\phi_\lambda$ (mole einstein <sup>-1</sup> ) | $\alpha^{Fe^{+3}}$ (cm <sup>2</sup> mole <sup>-1</sup> × 10 <sup>-3</sup> ) | $\kappa_{Fe^{+3}} \times L_R$ | $E_3(\kappa_{Fe^{+3}} L_R)^a$ |
|----------------|---|---|-------------------------------|-------------------------------|
| 275            | 1.24  | 4991.5  | 545.0                         | ≅0                            |
| 305            | 1.24  | 4991.5  | 545.0                         | ≅0                            |
| 310            | 1.24  | 4991.5  | 545.0                         | ≅0                            |
| 324            | 1.23  | 3970.4  | 433.6                         | ≅0                            |
| 359            | 1.14  | 1903.3  | 207.8                         | ≅0                            |
| 370            | 1.14  | 1406.1  | 153.5                         | ≅0                            |
| 385            | 1.14  | 953.9   | 104.2                         | ≅0                            |
| 410            | 1.09  | 338.8   | 33.7                          | ≅0                            |
| 423            | 1.04  | 162.2   | 18.3                          | ≅0                            |
| 436            | 1.01  | 103.6   | 2.82                          | 1.13 × 10 <sup>-02</sup>      |
| 490            | 0.94  | 2.44  | 0.29                          | 3.05 × 10 <sup>-01</sup>      |
| 523            | 0.59  | 0.49  | 0.05                          | 4.55 × 10 <sup>-01</sup>      |
| 545            | 0.15  | 0.27  | 0.03                          | 4.72 × 10 <sup>-01</sup>      |
| 580            | 0.013   | 0.55  | 0.06                          | 4.47 × 10 <sup>-01</sup>      |

<sup>a</sup> Values taken from Özisik [15].

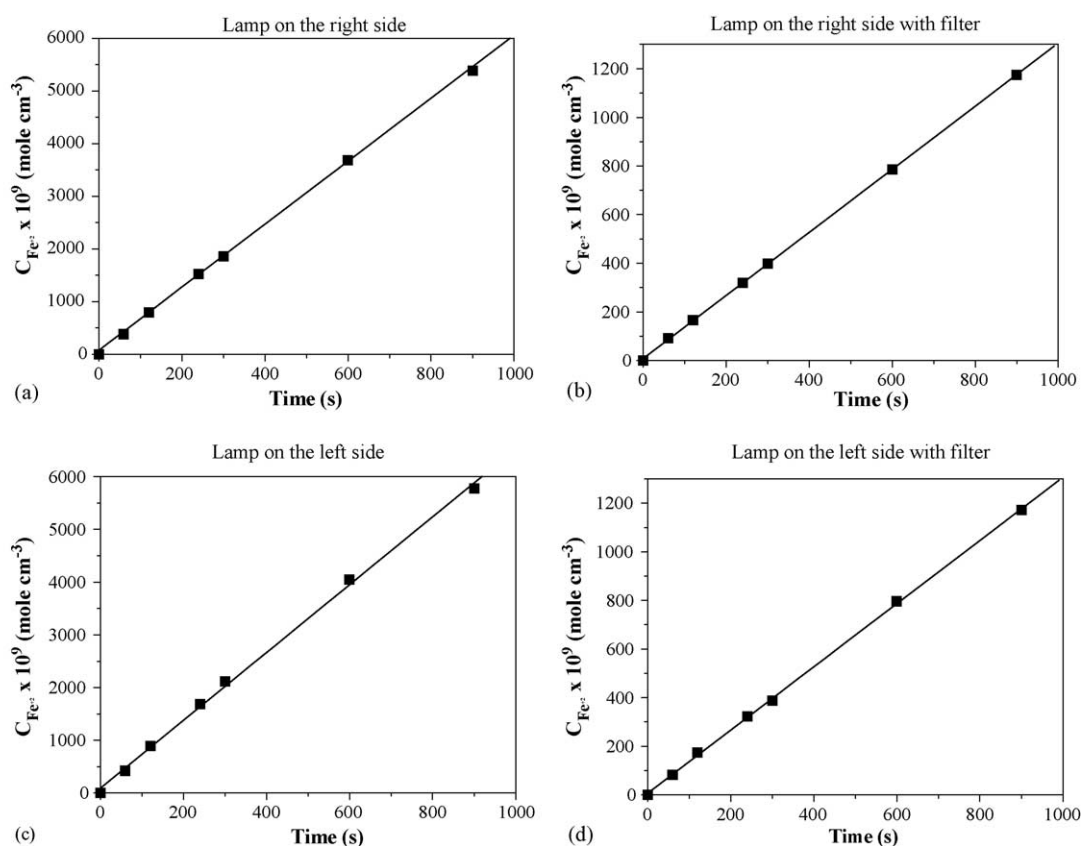


Fig. 6. Experimental actinometric results: (a) lamp on the right side, (b) lamp on the right side with filter, (d) lamp on the left side and (c) lamp on the left side with filter.

Table 3  
Experimental results

| Condition                                | Slope × 10 <sup>9</sup><br>(mole cm <sup>-3</sup> s <sup>-1</sup> ) |
|--|---|
| Lamp on the right side (100%)            | 6.03  |
| Lamp on the left side (100%)             | 6.43  |
| Lamp on the right side with filter (20%) | 1.30  |
| Lamp on the left side with filter (20%)  | 1.30  |

Table 4  
Incident radiation for each condition

| Lamp                         | G <sub>Tot,w</sub> × 10 <sup>6</sup><br>(einstein cm <sup>-2</sup> s <sup>-1</sup> ) |
|------------------------------|--|
| Right side (100%)            | 1.730  |
| Left side (100%)             | 1.840  |
| Right side with filter (20%) | 0.373  |
| Left side with filter (20%)  | 0.372  |



Table 5  
Boundary conditions as a function of wavelength

| Wavelength (nm) | $I_{\lambda}^0 \times 10^9$ (einstein $\text{cm}^{-2} \text{s}^{-1} \text{sr}^{-1}$ ) |                         |                                     |                                    |
|-----------------|---|-------------------------|-------------------------------------|------------------------------------|
|                 | Lamp  |                         |                                     |                                    |
|                 | On the right side (100%)  | On the left side (100%) | On the right side with filter (20%) | On the left side with filter (20%) |
| 275             | 2.85  | 3.04                    | 0.616                               | 0.614                              |
| 305             | 11.9  | 12.7                    | 2.56                                | 2.56                               |
| 315             | 14.5  | 15.4                    | 3.12                                | 3.12                               |
| 325             | 9.07  | 9.68                    | 1.96                                | 1.96                               |
| 359             | 23.4  | 25.0                    | 5.06                                | 5.05                               |
| 370             | 38.4  | 40.9                    | 8.29                                | 8.26                               |
| 385             | 28.8  | 30.7                    | 6.21                                | 6.19                               |

range between 275 and 385 nm, required to integrate the RTE in the photocatalytic system with titanium dioxide are shown in Table 5.

## 8. Conclusions

1. Actinometric measurements are a very powerful tool to calculate the exact boundary condition to integrate the radiative transfer equation in laboratory photochemical reactors for homogeneous systems.
2. When applied to a different homogeneous photochemical system, the result produced by the actinometer can be used to make precise calculations of the local values of the absorbed radiation energy in each point inside the reactor. In these cases, the same form of the radiative transfer equation must be used.
3. These results are required to develop precise kinetic models.
4. When these types of results are obtained for heterogeneous systems, they have the same importance in laboratory reactors. They permit to calculate the boundary condition for integrating the RTE in photochemical systems with absorption and scattering (slurry reactors for example) and thus calculate the exact value of the LVRPA at each point inside the reaction space and hence providing the exact information for accurate kinetic models.
5. All calculations of the reaction rates in well mixed reactors must be volume-averaged because experimental measurements are the result of concentrations measurements that, in well mixed reactors, are averaged values.

## Acknowledgements

Thanks are given to Universidad Nacional del Litoral, FONCYT (BID 1201/OC-AR) and CONICET for financial help. The doctoral fellowships of C.S.Z. and M.D.L. from CONICET are also acknowledged. The technical assistance of Eng. Claudia Romani is gratefully appreciated.

## References

- [1] W. Noyes, P. Leighton, *Photochemistry of Gases*, Reinhold, New York, 1941.
- [2] J. Calvert, J. Pitts, *Photochemistry*, Wiley, New York, 1966.
- [3] J. Rabek, *Experimental Methods in Photochemistry and Photo-physics*, Wiley, New York, 1982.
- [4] A. Braun, M. Maurette, E. Oliveros, *Technologie Photochemique*, first ed., Presses Polytechniques Romandes, Lausanne, 1986.
- [5] S. Murov, I. Carmichael, G. Hug, *Handbook of Photochemistry*, second ed., Marcel Dekker, New York, 1993.
- [6] W. Leighton, G. Forbes, Precision actinometry with uranyl oxalate, *J. Am. Chem. Soc.* 52 (1930) 3139–3152.
- [7] F. Parkhurst Brackett Jr., G. Forbes, Actinometry with uranyl oxalate at 278, 253 and 208 m $\mu$ , including a comparison of periodically intermittent and continuous radiation, *J. Am. Chem. Soc.* 55 (1933) 4459–4468.
- [8] G. Forbes, L. Heidt, Optimum composition of uranyl oxalate solutions for actinometry, *J. Am. Chem. Soc.* 56 (1934) 2363–2365.
- [9] D. Volman, J. Seed, The photochemistry of uranyl oxalate, *J. Am. Chem. Soc.* 86 (1964) 5095–5098.
- [10] L. Heidt, G. Tregay, A. Middleton Jr., Influence of pH upon the photolysis of the uranyl oxalate actinometer system, *J. Phys. Chem.* 9 (1970) 1876–1882.
- [11] C. Parker, A new sensitive chemical actinometer I. Some trials with potassium ferrioxalate., *Proc. Roy. Soc., A* 220 (1953) 104–116.
- [12] C. Hatchard, C. Parker, A new sensitive chemical actinometer II. Potassium ferrioxalate as a standard chemical actinometer., *Proc. Roy. Soc., A* 235 (1956) 518–536.
- [13] J. Lee, H. Seliger, Quantum yield of the ferrioxalate actinometer, *J. Phys. Chem.* 40 (1964) 519–523.
- [14] A. Cassano, C. Martín, R. Brandi, O. Alfano, Photoreactor analysis and design: fundamentals and applications, *Ind. Eng. Chem. Res.* 34 (1995) 2155–2201.
- [15] M. Özisik, *Radiative Transfer and Interactions with Conduction and Convection*, Wiley, New York, 1973.
- [16] O. Alfano, R. Romero, A. Cassano, A cylindrical photoreactor irradiated from the bottom-I. Radiation flux density generated by a tubular source and a parabolic reflector, *Chem. Eng. Sci.* 40 (1985) 2119–2127.
- [17] O. Alfano, R. Romero, A. Cassano, A cylindrical photoreactor irradiated from the bottom-II. Models for the local volumetric rate of energy absorption with polychromatic radiation and their evaluation, *Chem. Eng. Sci.* 41 (1986) 1115–1161.
- [18] O. Alfano, R. Romero, A. Cassano, A cylindrical photoreactor irradiated from the bottom-III. Measurement of absolute values of the local volumetric rate of energy absorption. Experiments with polychromatic radiation, *Chem. Eng. Sci.* 41 (1986) 1163–1169.

- [19] M. Clariá, H. Irazoqui, A. Cassano, A priori design of a photoreactor for the chlorination of ethane, *AIChE J.* 34 (1988) 366–382.
- [20] M. Cabrera, O. Alfano, A. Cassano, A novel reactor for photocatalytic kinetic studies, *Ind. Eng. Chem. Res.* 33 (1994) 3031–3042.
- [21] C. Martín, O. Alfano, A. Cassano, Decolorization of water for domestic supply employing UV radiation and hydrogen peroxide, *Catal. Today* 60 (2000) 119–127.
- [22] O. Alfano, A. Negro, M. Cabrera, A. Cassano, Scattering effects produced by inert particles in photochemical reactors. I. Model and experimental verification, *Ind. Eng. Chem. Res.* 34 (1995) 488–499.
- [23] R. Brandi, M. Citroni, O. Alfano, A. Cassano, Absolute quantum yields in photocatalytic slurry reactors, *Chem. Eng. Sci.* 58 (2003) 979–985.
- [24] R. Siegel, J. Howell, *Thermal Radiation Heat Transfer*, third ed., Hemisphere, Washington, DC, 1992.
- [25] C. Zalazar, Doctoral Thesis, Universidad Nacional del Litoral, Argentina, 2004.